Paper No. 558. (quote when citing this article)
Eleventh World Conference on Earthquake Engineering
ISBN: 0 08 042822 3

THE ROLE OF COMPUTATIONAL CONTINUUM MECHANICS IN STRUCTURAL CONTROL

G.F. DARGUSH and T.T. SOONG

Department of Civil Engineering
State University of New York at Buffalo
Buffalo, NY 14260 USA

ABSTRACT

The development of control devices and systems for civil structures has been based primarily upon a build-and-test approach. In this paper, the potential benefits of also employing a computational mechanics approach for the design and development of these critical elements in modern protective systems is explored. To illustrate the approach three specific device types are examined, including passive viscoelastic fluid dampers and metallic plate dampers, and active piezoelectric composite elements. The computational approach is used to characterize the overall force-deformation response for each of these devices. In the process, additional information is also obtained that is often useful for design purposes, including estimates of durability and, in some cases, feasibility of a given design concept. Consequently, it would appear that an increased emphasis on a computational mechanics-based approach would prove beneficial to the successful implementation of structural control technology.

KEYWORDS

Structural control; passive energy dissipation; viscoelastic fluid dampers; metallic dampers; piezoelectric materials; boundary element methods

INTRODUCTION

In recent years, considerable advancements have been made in the development of devices and systems for the passive or active control of civil engineering structures. This progress has been achieved by following a program that relies primarily upon physical experimentation. In particular, a build-and-test approach has generally been adopted for device development. The macroscopic force-deformation models, required for use in an overall structural analysis, are then constructed directly from experimental data which must be obtained for each specific device configuration. Device durability, and, in some cases, feasibility are also evaluated on the basis of laboratory testing. While the importance of quality physical experiments certainly cannot be questioned, the primary objective of this paper is to examine the potential benefits of also pursuing a computational mechanics-based approach for the design and development of these control devices.

The application of computational mechanics to three specific devices is discussed below in order to illustrate the utility of such an approach. Included in the presentation are investigations on a viscoelastic fluid damper, a triangular plate metallic damper, and a piezoelectric composite element. Distinct computational methodologies were developed specifically for each device. First, results from recent work on a viscoelastic fluid damper

(Makris *et al.*, 1993, 1995) are reviewed. For this case, a boundary element method was developed to characterize the dynamic stiffness of the device. Next, the response of a triangular plate metallic damper is examined by employing a simple finite deformation beam idealization, together with a two-surface constitutive model for structural steel under stabilized cyclic loading (Dargush and Soong, 1995). Finally, the behavior of a proposed piezoelectric composite element for structural applications is studied through the development of a quasistatic boundary element formulation. After examining these three applications, some remarks are provided concerning seismic design and the potential benefits of complementing the present device design and development process with a computational mechanics approach.

COMPUTATIONAL MECHANICS APPROACH

Generic Process

While there is a wide range of materials and geometric configurations that are applicable for structural control devices, an analysis of the performance based upon a computational mechanics approach can be viewed as a generic process. The following stages can be identified in this process: problem definition; constitutive modeling; theoretical formulation; numerical implementation; numerical analysis; design implications. However quite distinct computational methods will typically be required for each particular device type, as will be seen in the following examples.

Viscoelastic Fluid Damper

As a first example, consider the cylindrical pot viscoelastic fluid damper illustrated in Fig. 1 that has been studied in Makris *et al.* (1993, 1995) from a computational mechanics perspective. The damper consists of inner and outer stationary cylinders of radii r_3 and r_2, respectively, with a moving hollow cylindrical piston of intermediate radius r_1. A polybutane fluid occupies the space between the inner stationary cylinder and the piston as well as the space between the moving piston and the outer cylindrical boundary of the damper. With reference to Fig. 1, the geometric dimensions of GERB damper Type RHY-40/V50/H50 are: $r_1 = 0.084$m, $r_2 = 0.150$m, $r_3 = 0.018$m, $H_1 = 0.230$m, $H_2 = 0.060$m, and $H = 0.370$m.

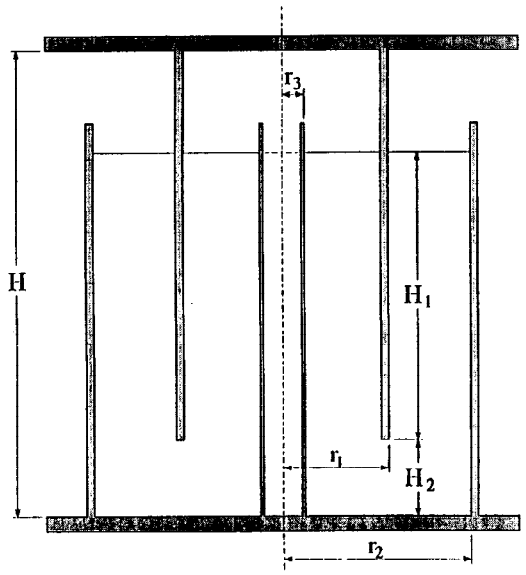

Fig. 1 Viscoelastic fluid damper geometric definition

For harmonic input, the dynamic stiffness of the damper is the ratio of the amplitude of the resulting force P_0 to the imposed displacement U_0. Accordingly, the dynamic stiffness of the device is $K^* = P_0/U_0$. A complete description of K^*, in terms of the stiffness magnitude and phase angle, as a function of the frequency can be used to characterize damper behavior under general time-dependent excitation.

The usual approach followed in the structural control literature involves determination of the dynamic stiffness directly from physical experiments on the damper. In fact, a series of such tests was conducted to measure this response. In each test, the damper piston was subjected to either vertical (axial) or horizontal (lateral) motion of specific amplitude and frequency. The storage and loss stiffnesses of the damper were then determined from records of the force needed to maintain the imposed motion by assuming linear steady-state behavior.

Alternatively, in Makris *et al.* (1995), a computational mechanics based approach was developed. A complex-derivative Maxwell constitutive model was used to characterize the polybutane fluid over a broad frequency and temperature range. At any reference temperature T_0, under the assumption of infinitesimal incompressible deformation, a scalar version of the model can be written:

$$\tau + [\lambda(T_0)]^{\nu} \frac{d^{\nu}\tau}{dt^{\nu}} = \mu(T_0)\gamma\,, \tag{1}$$

where τ and γ represent the shear stress and strain rate, respectively, while λ, ν, and μ are complex-valued material parameters. As indicated, both λ and μ are functions of temperature, and the symbol d^{ν}/dt^{ν} denotes a generalized derivative of order ν with respect to time. A Marquardt algorithm was used to determine all of the required material parameters from cone-and-plate viscometric test data.

The linearity of the applicable governing equations makes the boundary element method (BEM) an attractive approach for the numerical solution of this problem. Using the governing equations, along with an appropriate reciprocal theorem, the following integral representation can be established for excitation at frequency ω:

$$C_{ij}(\xi)v_i(\xi;\omega) = \int_S [G_{ij}(x,\xi;\omega)t_i(x;\omega) - F_{ij}(x,\xi;\omega)v_i(x;\omega)]dS(x)\,, \tag{2}$$

where the integration is performed over the bounding surface S of the damper fluid. In the above equation, v_i is the velocity, while t_i represents the surface traction. The point ξ is the location at which the velocity is determined, whereas x identifies the integration point which varies all along the surface of the body. The kernel functions G_{ij} and F_{ij} are derived from the infinite space fundamental solutions of the governing equations, which include the inertial contributions. The remaining constant tensor C_{ij} depends only upon the local geometry at ξ. It should be noted that Eq. (2) involves surface velocities and tractions only. Volume integration has been completely eliminated. Consequently, a boundary element analysis requires a mesh only on the surface S. Details of the formulation can be found in Makris *et al.* (1993, 1995).

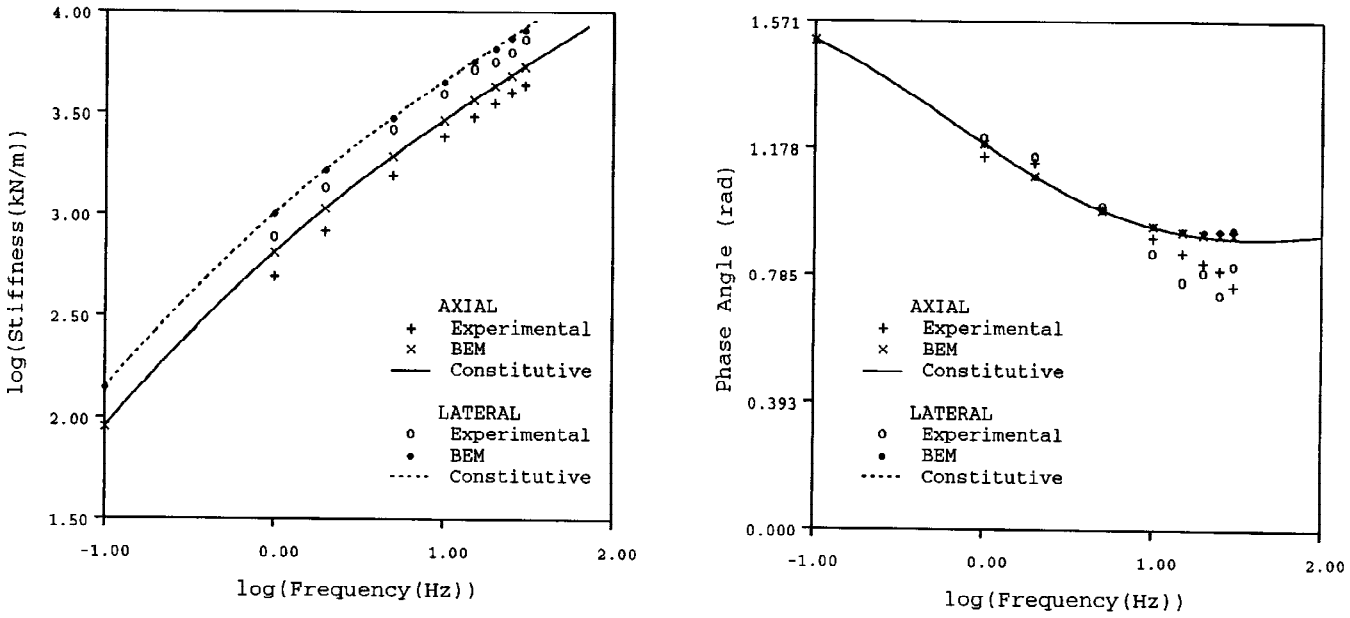

Fig. 2 Viscoelastic fluid damper frequency response. a) magnitude; b) phase angle

Numerical results obtained from the developed boundary element method for the viscous fluid damper are displayed in Fig. 2, along with the data obtained from physical experiments. The correlation is quite good throughout most of the frequency range 0-30Hz. However, the computational model tends to overpredict the magnitude of the device stiffness, and at the higher end of that range, the phase angle is also somewhat in error. While errors of this order may not be significant for design purposes, it is useful to attempt to identify their origin. It appears that the as-built dampers do not dissipate as much energy as theoretically possible under idealized linear behavior. This may be due to imperfect contact between the fluid and damper, to nonisothermal straining, or to localized finite deformation effects for which the present method does not account.

Figure 2 also contains curves obtained from a simplified computational approach in which a zero-frequency boundary element analysis is combined with the frequency variation inherent in the complex-derivative Maxwell constitutive model. The close correspondence between these curves and the dynamic BEM data points indicates that inertial effects are negligible in the frequency range of interest and that use of the simplified approach is appropriate.

Metallic Plate Damper

Metallic plate dampers, when incorporated into a structure, provide one of the most effective energy dissipation mechanisms available during an earthquake. Increasingly, these devices are applied in the seismic retrofit of structures which are found to be deficient. The design of these devices, however, has been largely based upon experiments and macroscopic modeling. In order to gain more insight into the response behavior of metallic plate dampers, a microscopic mechanistic approach was developed in Dargush and Soong (1995), and is summarized below.

In particular, consider the triangular plate metallic damper as developed by Tsai *et al.* (1993), which consists of N identical triangular structural steel plates positioned in parallel and typically installed within a frame bay between a chevron brace and the overlying beam. The base of each triangular plate is welded into a rigid base plate to approximate a fixed end condition, while a slotted pin connection is employed at the apex to approximate free movement in the vertical direction. As a result of this configuration, the damper primarily resists horizontal forces P, associated with an interstory drift Δ, via uniform flexural deformation of the individual plates. Thus, it is appropriate to examine a single cantilevered plate of thickness h, length L, and base width w_0, subjected to a load P/N applied at its free end as detailed in Fig. 3. Note that coordinate axes x, y, z are defined on the undeformed midsurface of the plate.

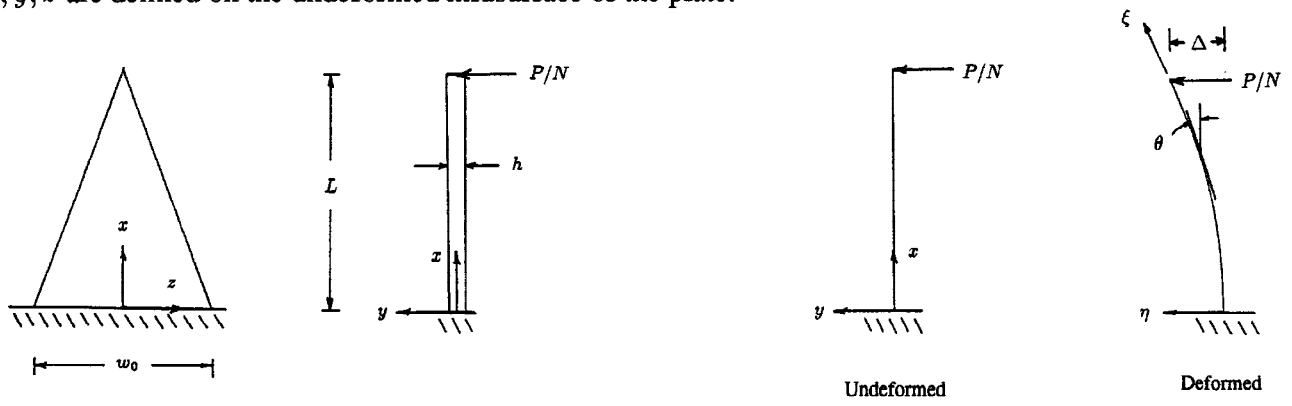

Fig. 3 Metallic plate damper problem definition.
a) geometric approximation; b) beam model

Under certain conditions (*e.g.*, major earthquakes), the interstory drift Δ may become comparable in magnitude to the damper plate length L. In these situations, the effects of finite deformation on damper response cannot be ignored. A simplified approach, which essentially involves writing the equation of moment equilibrium in the deformed configuration, is adopted. First an intrinsic ξ, η coordinate system is introduced, as shown in

Fig. 3, which deforms with the beam axis. Also defined in that diagram is θ, the angle between the x-axis and the tangent at ξ. As a simplification, the effects of shear deformation and the axial extension of the midsurface are ignored. Then, strictly from kinematic considerations,

$$\theta(\xi) = \int_0^{\xi} \kappa d\bar{\xi}\,; \qquad x(\xi) = \int_0^{\xi} \cos\theta d\bar{\xi}\,; \qquad y(\xi) = \int_0^{\xi} \sin\theta d\bar{\xi}\,, \tag{3a,b,c}$$

$$\epsilon = \kappa\eta\,. \tag{3d}$$

With finite deformation, the curvature κ is no longer constant along the length of the plate. Consequently, at each instant of time, a nonlinear boundary value problem (BVP) must be solved to determine the unknown curvature function. This BVP requires satisfaction of the moment equilibrium equation

$$\frac{P}{N}(x(L) - x(\xi)) = \frac{w_0(L-\xi)}{L} \int_{-h/2}^{+h/2} \sigma\eta d\eta\,, \tag{4}$$

which now varies with ξ. In addition, the free end deflection condition $y(L) = \Delta$ must be accommodated.

In establishing the stress σ in Eq. (4), a nonlinear constitutive model for structural steel must be employed. For this application a two-surface model with both kinematic and isotropic hardening is developed to represent behavior under stabilized cyclic conditions. Details are provided in Dargush and Soong (1995). An approximate numerical solution of the BVP can be obtained by collocating at a small number of nodes along the beam axis. The solution consists of the nodal values of the curvature and the total force P for a specified enforced displacement Δ. The response is, of course, history dependent due to the material nonlinearity.

For a specific example, consider the triangular plate damper 2B2 studied by Tsai *et al.* (1993), with $N = 8$, $h = 36.1$mm, $L = 304$mm, and $w_0 = 133.3$mm. Experimental results are presented in Fig. 4a for a cyclically increasing displacement-controlled component test. The pseudoangle γ in that diagram represents Δ/L. For the numerical simulation, constitutive model parameters were determined from the data presented by Cofie and Krawinkler (1985) for cyclic response of structural steel. The resulting force-displacement response prediction for the cyclic loading is provided in Fig. 4b, plotted to the same scale as the experimental data. Notice that the shapes of the hysteresis loops are quite similar, and that the estimated force in the damper at $\gamma = 0.30$ is within 15% of the measured value. Also of interest is the increasing stiffness of the device that becomes apparent for $\gamma > 0.20$. This is due to the effects of finite deformation, which become ever more significant as γ increases.

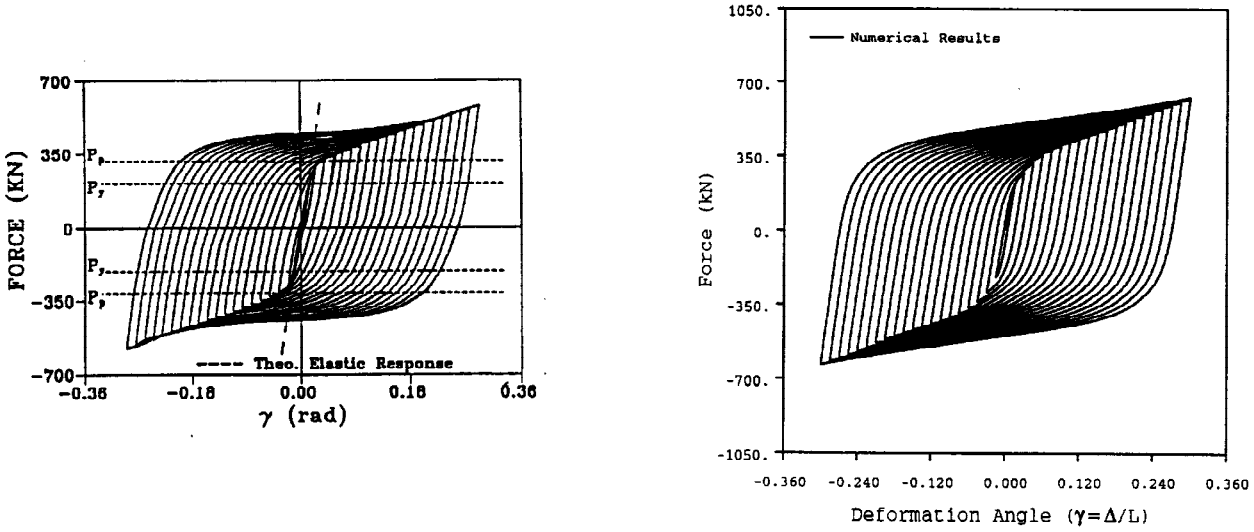

Fig. 4 Metallic plate damper cyclic response for specimen 2B2.
a) experimental (Tsai *et al.*, 1993); b) numerical

The numerical model also provides information concerning inelastic strain histories that can be used to estimate fatigue life under quasistatic conditions. The traditional approach for low-cycle fatigue analysis utilizes results of uniaxial tests run to failure at various levels of the cyclic strain range. For a wide range of metals, the relationship between the plastic strain amplitude ($\Delta\epsilon_p/2$) and the number of strain reversals to failure ($2N_f$) approximates a power law. This so-called Coffin-Manson relationship can be used, in conjunction with low-cycle fatigue data compiled by Boller and Seeger (1987) to estimate fatigue life. From an analysis of damper 2B2 with a constant cyclic displacement amplitude of 55mm corresponding to $\gamma = 0.18$, the maximum inelastic strain range is approximately $\Delta\epsilon_p = 0.04$. The predicted life is approximately 35 cycles. This simple approach appears to provide at least a reasonable order-of-magnitude guide to anticipated life, which could be useful in preliminary damper design. Additionally, it should be recognized that plastic strain range is the key parameter in determining damper durability, not the macroscopic variables P and γ. Additional information is provided in Dargush and Soong (1995).

Piezoelectric Composite Element

As a final example, consider a piezoelectric composite element for potential application in an active structural control system. Two different design concepts, involving extension-type and shear-type piezoelectric layers, are illustrated in Fig. 5. A preliminary investigation, utilizing typical beam assumptions, indicated that the shear-type composite element might provide some distinct advantages, however a more detailed continuum mechanics analysis was in order to assess the feasibility of these members for civil structural applications.

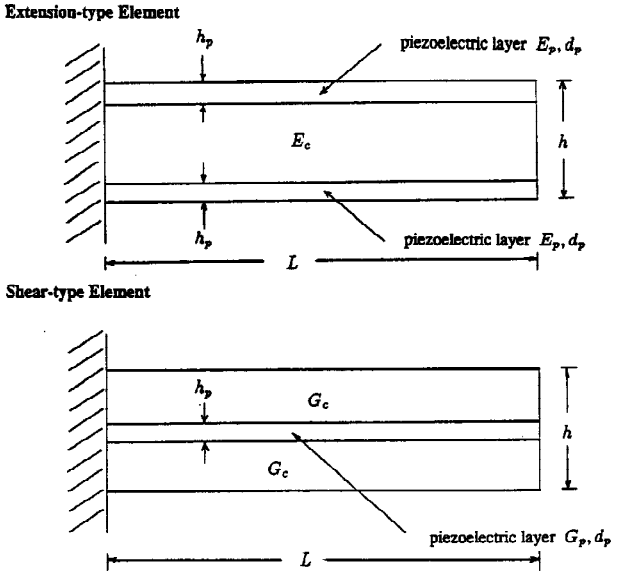

Fig. 5 Piezoelectric composite element geometric definition.

Since the later stages of the 19th century, it has been known that materials of certain symmetry classes exhibit a direct piezoelectric effect in which an electric polarization is produced by and in proportion to a mechanical strain. On the other hand, the converse piezoelectric effect concerns the development of strains in proportion to an applied electric polarization. For the converse case, the constitutive model for a piezoelectric material, undergoing infinitesimal deformation, can be written (Cady, 1946):

$$\sigma_{ij} = c_{ijkl}(\epsilon_{kl} - d_{mkl}E_m)\,, \tag{5}$$

where σ_{ij} and ϵ_{ij} are the stress and strain tensors, respectively, and the electric field $E_i = \phi_{,i}$ with ϕ representing the electric potential and the comma symbolizing differentiation with respect to spatial coordinates. Additionally, c_{ijkl} is the usual elasticity tensor, while d_{ijk} are the piezoelectric constants that determine the coupling between the electric and deformation fields.

Notice that the form of Eq. (5) is similar to that for the more familiar thermoelasticity theory, except that the coupling in Eq. (5) involves a third order tensor d_{ijk} rather than a second order tensor of thermal expansion coefficients. The third order nature of this coupling tensor precludes the appearance of piezoelectric effects in materials belonging to many high symmetry classes. For example, isotropic materials cannot exhibit piezoelectric behavior. Naturally occurring piezoelectric materials include quartz and Rochelle salt, while many engineering applications utilize synthetic piezoelectric polymers (*e.g.*, PVDT) or ceramics (*e.g.*, PZT).

A boundary element formulation can be developed for the piezoelectric composite members shown in Fig. 5 in the following manner. First rewrite Eq. (5) in the form:

$$\sigma_{ij} = \sigma^c_{ij} - \sigma^o_{ij}\,, \tag{6}$$

with $\sigma^c_{ij} = c_{ijkl}\epsilon_{kl}$ and initial stress $\sigma^o_{ij} = c_{ijkl}d_{mkl}E_m$. Then, consideration of equilibrium yields

$$\sigma^c_{ij,j} + f^o_i = 0\,, \tag{7}$$

with $f^o_i = \sigma^o_{ij,j}$. Utilizing the Betti reciprocal theorem, the boundary integral representation for the displacement u_i becomes

$$C_{ij}(\xi)u_i(\xi) = \int_S [G_{ij}(x,\xi)t^c_i(x) - F_{ij}(x,\xi)u_i(x)]dS(x) + \int_V [G_{ij}(x,\xi)f^o_i(x)]dV(x)\,, \tag{8}$$

where G_{ij} and F_{ij} are the anisotropic elastic kernel functions, and t^c_i is the traction associated with σ^c_{ij}. As in Eq. (2), ξ and x represent the collocation and integration points, respectively, while the tensor C_{ij} depends upon the local geometry. Finally, assuming that the electric field is constant within each piezoelectric layer, the following boundary-only formulation obtains:

$$C_{ij}(\xi)u_i(\xi) = \int_S [G_{ij}(x,\xi)t_i(x) - F_{ij}(x,\xi)u_i(x)]dS(x) + \sigma^o_{ik}\int_S [G_{ij}(x,\xi)n_k(x)]dS(x)\,, \tag{9}$$

and a multiregion BEM can be readily constructed for the composite elements shown in Fig. 5. In Eq. (9), n_k represents the outward normal vector to the surface $S(x)$.

Results of a comparative nondimensional BEM analysis of the two different design concepts is provided in Fig. 6. The deformed shapes obtained, using relative material properties for the extension and shear-type

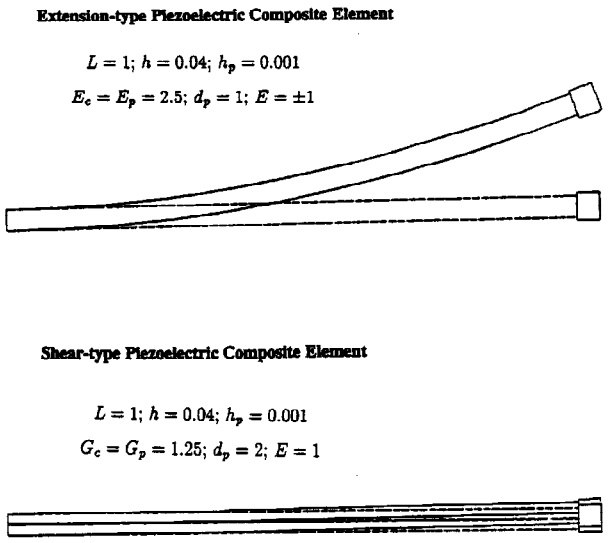

Fig. 6 Piezoelectric composite element deformation response.

piezoelectric layers based upon typical PZT values, indicate the clear superiority of the extension-type concept. Close examination of the shear-type composite element response reveals that plane sections do not remain plane after deformation, and thus the preliminary investigation based upon beam bending behavior is invalid.

In addition, however, the feasibility of even the more favorable extension-type element must be examined. Although PZT piezoelectric ceramics are very effective transducers of electrical energy input into mechanical work, the present technology limits the electric field E_i and piezoelectric strain $d_{kij}E_k$ in such materials to approximately 20kV/cm and 0.001, respectively. This severely restricts the potential of PZT ceramics in civil structural applications. In particular, relatively thin piezoelectric layers will not have sufficient stiffness to control the relevant deflections in typical structural members.

CONCLUDING REMARKS

For each of the three cases discussed above, the objective of the analysis is not only to develop a macroscopic model suitable for design purposes, but also to utilize the method to gain further insight into anticipated device behavior. For example, dynamic stiffnesses obtained from the numerical analyses of the viscoelastic fluid damper correlate quite well with those determined via physical measurement. In addition, the analysis suggests that some attention should be directed toward possible slippage along fluid-solid interfaces. In the triangular plate metallic damper, good agreement is again obtained with experimental data, but useful information is also provided concerning durability. In the third application area, proposed piezoelectric composite element designs, involving extensional and shear modes, are compared, and then evaluated for application in large-scale structures.

In a structure designed or retrofitted with a seismic protection system, the safety of the structure and its occupants depends to a significant degree upon the performance of the control devices. Thus, these devices become critical elements in the overall structural system, and should receive a significant amount of engineering attention, particularly when new materials or technologies are involved. Meanwhile, it has been illustrated that a detailed computational mechanics investigation of passive or active control devices can almost certainly lead to a better understanding of their anticipated structural response. For the three dampers considered here, this approach also resulted in the development of models for macroscopic device performance, and the identification of several outstanding design issues. Based upon the results of these studies, and in light of the critical nature of seismic protection systems, it would appear that an increased emphasis on a computational mechanics-based approach would prove beneficial to the successful implementation of structural control technology.

REFERENCES

Boller, Chr. and Seeger, T. (1987). *Material Data for Cyclic Loading*. Elsevier, Amsterdam.

Cady, W.G. (1946). *Piezoelectricity*. McGraw-Hill, New York.

Cofie, N.G. and Krawinkler, H. (1985). Uniaxial cyclic stress-strain behavior of structural steel. *J. Engrg. Mech.*, ASCE, **111**, 1105-1120.

Dargush, G.F. and Soong, T.T. (1995). Behavior of metallic plate dampers in seismic passive energy dissipation systems. *Earthquake Spectra*, **11**, 545-568.

Makris, N., Dargush, G.F. and Constantinou, M.C. (1993). Dynamic analysis of generalized viscoelastic fluids. *J. Engrg. Mech.*, ASCE, **119**, 1663-1679.

Makris, N., Dargush, G.F. and Constantinou, M.C. (1995). Dynamic analysis of viscoelastic fluid dampers. *J. Engrg. Mech.*, ASCE, **121**, 1114-1121.

Tsai, K.C., Chen, H.W., Hong, C.P. and Su, Y.F. (1993). Design of steel triangular plate energy absorbers for seismic-resistant construction. *Earthquake Spectra*, **9**, 505-528.